

SUPPLEMENTARY MATERIAL for

Two-band Conduction and Nesting Instabilities in in Superconducting $\text{Ba}_2\text{CuO}_{3+\delta}$: a First Principles Study

Hyo-Sun Jin¹, Warren E. Pickett^{2,*} and Kwan-Woo Lee^{1,3†}

¹*Division of Display and Semiconductor Physics, Korea University, Sejong 30019, Korea*

²*Department of Physics, University of California, Davis, CA 95616, USA*

³*Department of Applied Physics, Graduate School, Korea University, Sejong 30019, Korea*

(Dated: May 27, 2021)

We provide here following additional information.

Section I. Comparison of band structures of the antiferromagnetic (AFM) ordered $\delta = 0$ phase from two all-electron, full-potential codes of WIEN2K and FPLO, which show excellent agreement.

Section II. Effects of three $\vec{q}=0$ oxygen phonon modes on the energy gap and Cu local moment in the AFM $\delta = 0$ phase, indicating that the gap is more sensitive to a planar oxygen motion.

Section III. Additional data on structure optimization for the ordered defect structures at $\delta = 1/4$, providing information on the orthorhombic distortion and variations of Cu-O separations due to the ordered defects.

Section IV. Band structure and fatband plots of the energetically unfavored structures at $\delta = 1/4$, showing effects of the ordered O vacancies on the Cu $3d$ bands.

*Electronic address: wepickett@ucdavis.edu

†Electronic address: mckwan@korea.ac.kr

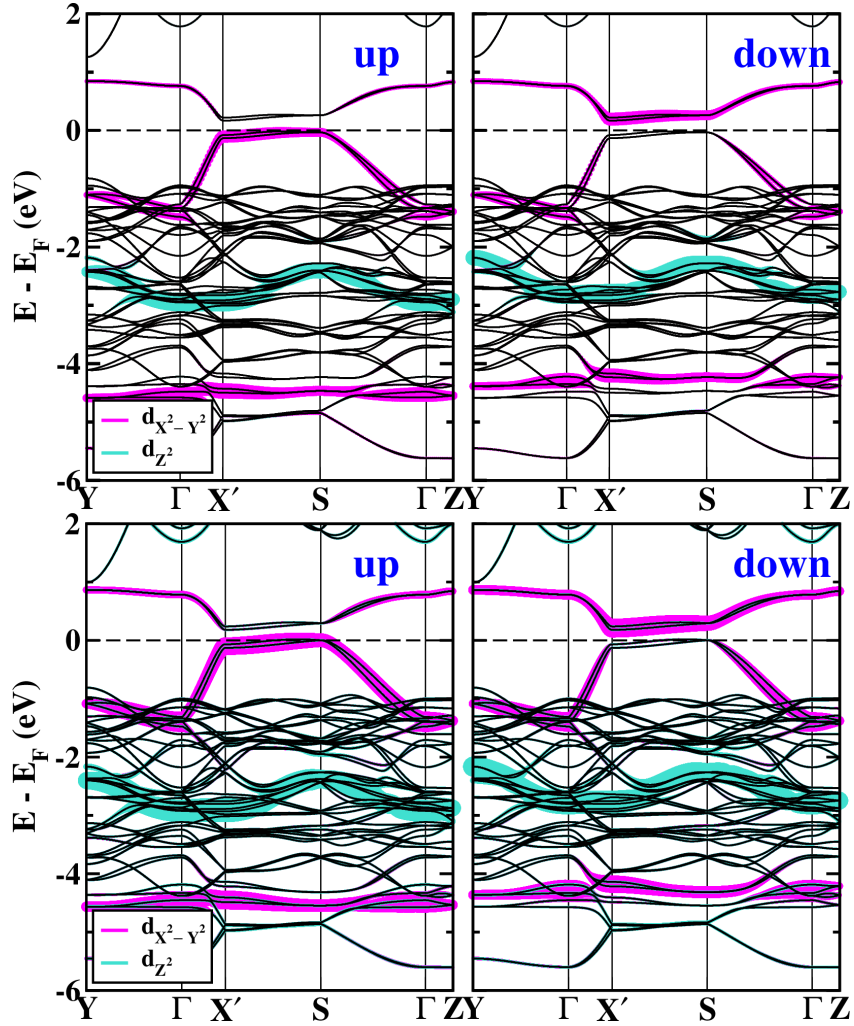


FIG. 1: Band structures for AFM Cu spin alignment in the $\delta = 0$ phase, obtained from FPLO (top panel), and from WIEN2K (bottom panel). The agreement is excellent.

I. BAND STRUCTURE OF THE AFM $\delta = 0$ PHASE: COMPARISON OF CODES

In the text we noted that WIEN2K [1] results for this system (and others) is almost the same as for another all-electron, full potential code FPLO [2] that we frequently use. Here we provide briefly an indication of the level of agreement of these two codes, with their very different basis sets and representation of wavefunctions and spin densities. This might become a question for some, since the gap open without Hubbard U in Ba_2CuO_3 whereas that rarely if ever happens in square lattice cuprates.

Figure 1 shows the level of agreement between the band structures of the two codes in the antiferromagnetic states for $\delta=0$; the bands for WIEN2K are practically identical to those of FPLO, which are reprinted here (from the main text) to allow more direct comparison. Even in this enlarged 4 eV range centered at the gap, no difference is apparent to the eye. Energy gaps in particular can be sensitive to the methods used and the approximations made in various electronic structure codes. The energy gap at, for instance, the S point differs by only 0.03 eV between these two codes.

At this close level of agreement the spin densities as well as the charge densities, which give rise to the potential, must be extremely close. Physical quantities can be difficult to compare. Just as the charge density cannot be decomposed objectively and uniquely into atomic parts, neither can the magnetic moments on the Cu ion (or O ions). Specifically, moments quoted by WIEN2K users are based on integrals within chosen atomic spheres. For FPLO, the spin densities are projected onto atomic-like basis functions to obtain a good (but not unique) measure of the “atomic moment.”

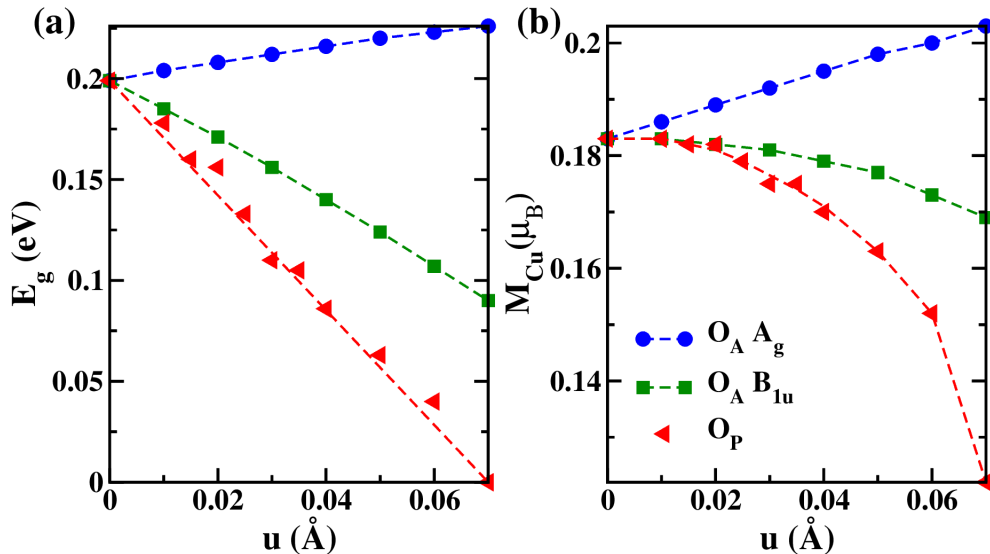


FIG. 2: Variations of (a) energy gap E_g and (b) Cu local moment M_{Cu} versus the O displacement u for the $O_A A_g$ and B_{1u} modes, and the O_P breathing mode. These are obtained for the AFM $\delta = 0$ phase.

II. EFFECTS OF OXYGEN PHONON MODES

Electron-lattice coupling has important effects in cuprate phenomena. The simplest O displacement modes, and the ones of most common interest, are the $O_A A_g$ and B_{1u} modes and the O_P breathing mode, and some results are provided here for the AFM ordered $\delta = 0$ structure. All are $\vec{q}=0$ in the AFM cell.

For the A_g (apical oxygen pinch) mode, both the AFM band gap E_g and Cu moment M_{Cu} increase linearly with increasing amplitude, whereas both monotonically decrease, much more rapidly, for the other two modes. The variations with amplitude of the O_P mode are the most substantial, with the Cu moment becoming quite supralinear. For this mode, at $u = 0.07 \text{ \AA}$ where the local moment has reduced by 1/3, the gap closes. Note that these displacement amplitudes are typical, if not actually smaller than, typical O optical modes in insulating oxides. These results indicate that the gap is more sensitive to planar O motion, and that this motion may be anharmonic.

TABLE I: Optimized lattice parameters and Cu-O separations (in units of \AA) for the three choices of ordered defect structures, shown in Fig. 2 of the main text, for $\delta = 1/4$. The bilayer structure is energetically favored over the other two. As in the main text, O_P and O_A denote the planar and apical oxygens, respectively. The notation $\text{Cu}N$ indicates the N -fold coordinated Cu site, with $\text{Cu}4^*$ denoting the 4-fold rung Cu site.

type	a	b	Cu- O_A				Cu- O_P			
			Cu6	Cu5	Cu4	Cu4*	Cu6	Cu5	Cu4	Cu4*
bilayer	4.15	3.84	2.00	–	1.90	1.93	2.32/1.92	–	2.08	1.84
monolayer	3.96	4.04	–	1.95	1.92	1.92	–	2.21/1.98	1.98	1.82
brickwall	4.05	3.93	–	1.98	1.92	–	–	2.02/1.96	2.02	–

III. ADDITIONAL DATA ON STRUCTURE OPTIMIZATION

One of the primary reasons for the recent activity on the study of $\text{Ba}_2\text{CuO}_{3+\delta}$ is its structure. A paradigm has been the long Cu- O_A separation compared to the in-plane separation, giving a characteristic crystal field that promotes hole occupation solely in the $d_{x^2-y^2}$ orbital, making cuprates at the basic level single-band materials. In Table I we provide calculated structural information, with focus on the Cu-O separations, for the three $\delta = 1/4$ structures that we have studied.

The original structural refinement of Ba_2CuO_3 for $\delta = 1/4$ imposed equal lattice constants $a = b$ as would be the case for random occupation, but was refined to an ordered orthorhombic structure. As we have noted, the

orthorhombicity does not (somewhat surprisingly) affect some properties much, and we reported only the $a = b$ structure in the main text.

Here we provide the optimized lattice parameters and Cu-O separations (in units of Å) for the three choices of ordered defect $\delta = 1/4$ structures; these are shown in Fig. 2 of the main text. The cell volume was fixed to that of the experimental values when optimizing. The optimized lattice parameters c are 12.98-13.04 Å. The results are given in Table I.

The difference in a and b lattice constants is least for the monolayer structure, equal to the average $\pm 1\%$. For the brickwall structure the difference is $\pm 1.5\%$, while those of the bilayer structure show the largest difference, almost $\pm 4\%$. In the bilayer and monolayer structures, the Cu6, respectively Cu5, O_P distances are longer along the rung (*i.e.*, Cu6 (Cu5)- O_P -Cu4*) direction, whereas all Cu5- O_P distances are similar in the high energy brickwall structure.

We summarize the main points. For the energetically favored bilayer structure, both the value $(a + b)/2 = 4.00$ Å and the ratio $a/b \approx 1.09$ are anomalously large, and apical heights 1.90–2.00 Å are anomalously small. Both the former and the latter are in broad agreement with the experimental structural values that surprised cuprate researchers. Another observation is that this structure and resulting local crystal fields brings d_{z^2} states closer to, in some cases actually at, the Fermi level. The smaller bandwidth implies that its participation in properties may be much different from that of the $d_{x^2-y^2}$ orbitals with their large $pd\sigma$ hopping amplitude.

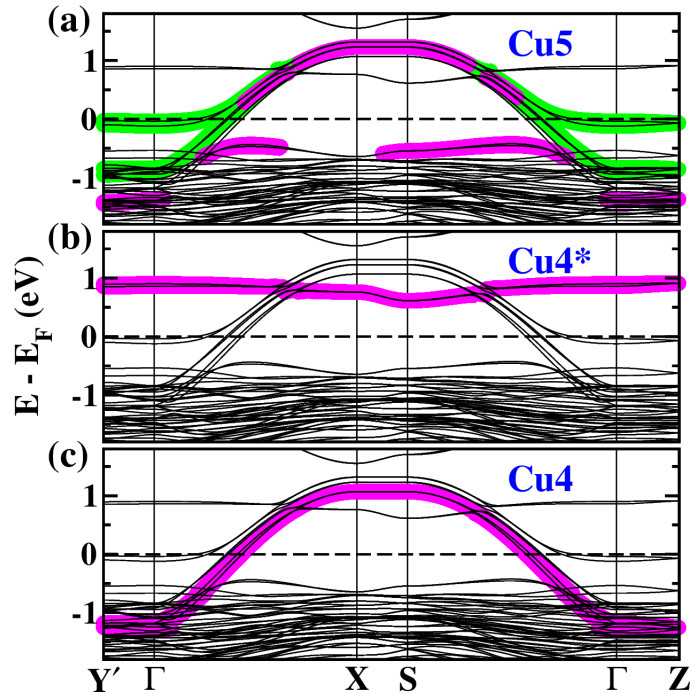


FIG. 3: Enlarged band structures of the nonmagnetic $\delta = 1/4$ monolayer phase in the range of -1.8 eV to 1.8 eV. The characters of the e_g orbitals of (a) Cu5, (b) Cu4*, and (c) Cu4 are highlighted by magenta ($d_{x^2-y^2}$ or $d_{X^2-Y^2}$) and green (d_z^2) colors. (Note: the band structure is identical in each panel, only the emphasis changes.)

IV. BAND STRUCTURES OF ENERGETICALLY UNPAIRED STRUCTURE IN $\delta = 1/4$

It may be important to know the main features of the ordered vacancy $\delta = 1/4$ structures, especially how they affect the Cu 3d states. Figure 3 presents the bands for the nonmagnetic monolayer structure. Dispersion across E_F occurs only along the $\Gamma - X'$ direction with participation of Cu4 and Cu5 $d_{x^2-y^2}$ or $d_{X^2-Y^2}$ orbitals (see the main text for notation). Most interesting is that a flat band arising from this orbital on the Cu5 site lies very slightly below E_F until it mixes with, and follows the dispersing orbitals to the maximum at the zone edge. Very unusually, the Cu4* site contributes a flat band at 1 eV for the same type of orbital. This empty band identifies this site as having a d^8 “highly hole-doped” configuration. The (three) Fermi surfaces can be viewed as electron barrels centered at Γ , or hole surfaces around the zone edge.

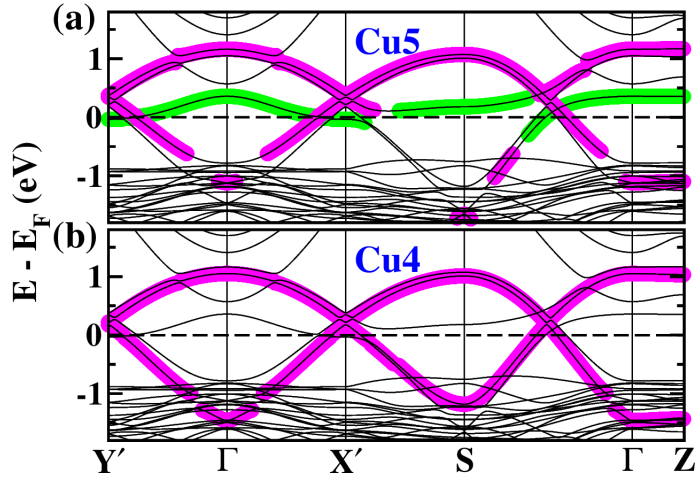


FIG. 4: Enlarged band structures of the nonmagnetic $\delta = 1/4$ brickwall phase in the range of -1.8 eV to 1.8 eV. The characters of the e_g orbitals of Cu5 and Cu4 are highlighted by colors as in Fig. 3.

A similar presentation for the brickwall structure is presented in Fig. 4, which a Brillouin zone of different shape. Degeneracies of Cu4 and Cu5 $d_{x^2-y^2}$ or $d_{X^2-Y^2}$ orbitals at X' and Y' are linked along the symmetry lines in oppositely directed cosine shaped bands shared by both orbitals. In addition, there is an empty flat Cu5 d_{z^2} band lying very close to E_F , this apparently being the counterpart of the flat band at E_F in the monolayer structure of Fig. 3. In this structure the periodicity conspires to put small hole surfaces at various places in the 2D one.

-
- [1] K. Schwarz and P. Blaha, Comput. Mater. Sci. **28**, 259 (2003).
[2] K. Koepnik and H. Eschrig, Phys. Rev. B **59**, 1743 (1999).